



PNA from an ordered chain to a random coil, a process that also reorients the fluorophore.

The mixed sequence PNAs form both parallel and antiparallel duplexes with appropriate complementary DNA sequences, with antiparallel duplexes being more stable than parallel duplexes.<sup>2</sup> The effect of incorporating *2ap* in place of A on the thermal stability of duplexes is seen from the UV absorbance–temperature data for PNA·DNA duplexes ( $T_m$ ; **5·6**, 25.5 °C; **5·7**, 25.0 °C; **4·6**, 28.0 °C; **4·7**, 28.5 °C). The single replacement of A by *2ap* caused a lowering of  $T_m$  by 2–3 °C for both parallel (N/5', **5·6**) and antiparallel (N/3', **5·7**) *2ap*-PNA·DNA duplexes as compared to the corresponding unmodified control duplexes **4·6** and **4·7** respectively. The data indicate a relatively large increase in fluorescence intensity (60%) of *2ap* in duplex with temperature as compared to that in *2ap*-PNA alone (25%). Further, a slight blue shift in emission maxima (2 nm) was noticed at 50 °C compared to that at 5 °C, indicating a more hydrophilic environment for *2ap* after melting. The fluorescence intensity showed a small decrease beyond 40 °C, similar to *2ap*-PNA (Fig. 1). The parallel PNA·DNA duplex (**5·6**) gave temperature dependent fluorescence spectra (not shown) similar to those of the antiparallel (**5·7**) duplex. Surprisingly, the decrease in fluorescence anisotropy (10%) of the *2ap* moiety in PNA upon PNA·DNA melting was less than that seen with *2ap*-PNA alone (45%).

The fluorescence  $T_m$  obtained from the data in Fig. 1 for *2ap*-PNA·DNA melting (**5·7**, 27.5 °C) was less by 5 °C than the  $T_m$  for self-melting of *2ap*-PNA (**5**, 32.5 °C), consistent with the general observation that the thermal stability of the PNA·DNA duplex is lower than that of PNA.<sup>2</sup> It is interesting, but not unprecedented,<sup>6a</sup> to note that the fluorescence  $T_m$  of the duplexes (**5·6**, 27.5 °C; **5·7**, 27.0 °C) were *ca.* 2.5 °C higher than the  $T_m$  of the corresponding duplexes derived from UV absorbance changes. This difference may arise from the fact that the UV equilibrium melting curves monitor the global duplex dissociation while the fluorescent melting curve monitors local duplex perturbations in the vicinity of the fluorophore.<sup>6</sup> The temperature dependent fluorescence data is also influenced by transient kinetic states that are not reflected in equilibrium data.

The kinetics of the PNA·DNA hybridization process were examined by monitoring the fluorescence emission decay at 367 nm as a function of time after mixing of *2ap*-PNA **5** with the complementary antiparallel DNA **7** (Fig. 2). The emission intensity decreased exponentially over a period of 6 min [Fig. 2, curve (c)] and thereafter remained constant. In contrast, either *2ap*-PNA **5** alone or its mixture with DNA dA<sub>10</sub>, **8** having three mismatches with PNA, did not exhibit any effect on the PNA fluorescence [Fig. 2, curves (a) and (b)]. The time-dependent decrease in fluorescence of **5** immediately upon mixing with **7** may therefore be attributed to specific formation of a *2ap*-PNA·DNA hybrid (**5·7**). Similar kinetic behaviour has been previously observed for PNA·PNA hybrid by monitoring the

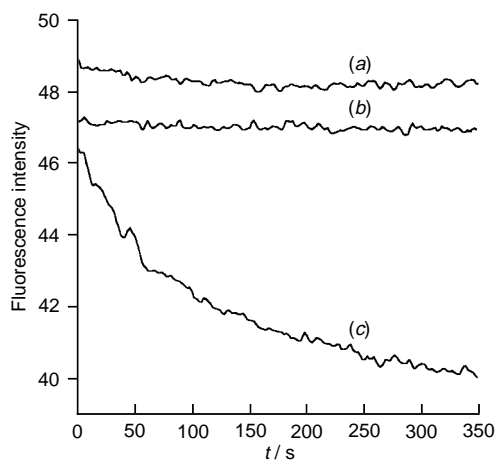


Fig. 2 Fluorescence decay kinetics at 15 °C monitored by emission at 365 nm: (a) **5**, (b) **5·8** and (c) **5·7**

evolution of a circular dichroism signal arising from helical propagation in a 10-mer lys-PNA upon mixing with a complementary PNA sequence<sup>8</sup> where signal saturation occurred at around 6 min. The decay profile observed could be fitted to a double exponential function with time constants of 46 and 290 s, indicating that the fluorescent base *2ap* in PNA monitors at least two types of local events, a fast duplex formation by complementary hydrogen bonding followed by a slow reorganization of the helix after duplex formation.

Structural studies of DNA/PNA using fluorescence are best performed without perturbing their structures, which is possible only with the use of intrinsic fluorescence from the base. In this context, *2ap* is an ideal fluorophore since it senses both steady state and dynamic conformational changes. The present results clearly demonstrate that *2ap* is easily accommodated in a PNA chain and the intrinsic fluorescence can be employed to monitor PNA self-melting and PNA·DNA duplex transitions. The anisotropy changes suggest that the *2ap* residue in a PNA chain is more ordered than its environment in a PNA·DNA duplex. Since *2ap* can be placed at any point in a PNA·DNA helix to monitor local events, the type of probes reported here have potential for studying the consequences of backbone modifications on the PNA self-structure and on PNA·DNA duplex. Apart from their utility in diagnostics, these PNA probes may be applicable to other areas, such as the study of cellular uptake and intracellular distribution of PNA by employing fluorescence microscopy, and as sequence specific DNA biosensors.<sup>9</sup>

## Footnotes and References

† E-mail: kng@ems.ncl.res.in

‡ Selected data for **2**:  $\delta_H$ (CDCl<sub>3</sub>) 8.65 (s, 1H, AH8), 7.93–7.90 (s, 1H, AH6), 5.80 (br s, 1H, NH), 5.40 (br s, 1H), 5.00–4.85 (s, 2H, glyCH<sub>2</sub>), 4.17–4.05 (s, 2H, N–CH<sub>2</sub>), 4.25 (m, 2H), 3.67–3.56 (m, 2H), 3.40–3.32 (m, 2H), 1.45 (s, 9H), 1.25 (m, 3H);  $\delta_C$ (CDCl<sub>3</sub>) 169.6–169.3 (CO<sub>2</sub>Et), 167.3–166.9 (CONH), 159.9 (C2), 156.2 (BocOCON), 153.4 (C8), 148.6 (C6), 143.7 (C4), 126.8 (C5), 79.7 (Me<sub>3</sub>CO), 62.1, 61.5, 48.4, 38.6, 28.3 (all CH<sub>2</sub>), 13.9 (Me<sub>3</sub>C). For **3**:  $\delta_H$ (D<sub>2</sub>O) 8.7 (s, 1H), 8.33 (s, 1H), 5.31 and 5.12 (s, 2H), 4.17 and 4.07 (s, 2H), 3.7 (t, 2H), 3.58 (t, 2H), 3.4 (t, 2H), 3.23 (t, 2H), 1.42 and 1.43 (s, 9H);  $\delta_C$ (CDCl<sub>3</sub>) 171.6–171.07 (CO<sub>2</sub>Et), 167.7–167.2 (CONH), 161.0 (C2), 156.3 (BocOCON), 153.9 (C6), 149.3 (C8), 143.9 (C4), 126.9 (C5), 78.7 (Me<sub>3</sub>CO), 50.2, 48.9, 47.6, 43.6, 28.7 (all CH<sub>2</sub>), 13.9 (Me<sub>3</sub>C).

§ RP 18 column; buffer A: 0.1% TFA in water, buffer B: 0.1% TFA in MeCN gradient 0–40% B in A in 30 min. R: **4**, 12.28 min; **5**, 12.26 min.

¶ Fluorescence spectra were recorded on a Perkin-Elmer LS 50B spectrometer, equipped with a flow cell and attached to a Julabo water circulator for variable temperature measurements, using a slit width of 5 nm. The PNA·DNA duplexes were constituted by mixing equimolar amounts of each strand (4  $\mu$ M) in 10 mM phosphate buffer (pH 7.0, 2 ml) followed by heating at 80 °C for 3 min, cooling to ambient temperature and storage at 4 °C overnight.

- P. E. Nielsen, *Annu. Rev. Biophys. Biomol. Struct.*, 1995, **24**, 167.
- B. Hyrup and P. E. Nielsen, *Bioorg. Med. Chem. Lett.*, 1996, **4**, 5.
- D. R. Corey, *Trends Biotechnol.*, 1997, **15**, 224.
- G. Haaima, A. Lohse, O. Buchardt and P. E. Nielsen, *Angew. Chem., Int. Ed. Engl.*, 1996, **35**, 1939; B. P. Gangamani, V. A. Kumar and K. N. Ganesh, *Tetrahedron*, 1996, **52**, 15 017.
- D. C. Ward, E. Reich and L. Stryer, *J. Biol. Chem.*, 1969, **244**, 1228.
- (a) D. Xu, K. O. Evans and T. M. Nordlund, *Biochemistry*, 1994, **33**, 9592; (b) S. M. Law, R. Eritja, M. F. Goodman and K. J. Breslauer, *Biochemistry*, 1996, **35**, 12 329; (c) D. P. Millar, *Curr. Opin. Struct. Biol.*, 1996, **6**, 322; (d) R. A. Hochstrasser, T. E. Carver, L. C. Sowers and D. P. Millar, *Biochemistry*, 1994, **33**, 11 971; (e) M. W. Frey, L. C. Sowers, D. P. Millar and S. J. Benkovic, *Biochemistry*, 1995, **34**, 9185.
- P. C. Meltzer, A. Y. Liang and P. Matsudaira, *J. Org. Chem.*, 1995, **60**, 4305.
- P. Wittung, M. Eriksson, R. Lyang, P. E. Nielsen and B. Norden, *J. Am. Chem. Soc.*, 1995, **117**, 10 167.
- J. Wang, E. Palecek, P. E. Nielsen, G. Rivas, X. Cai, H. Shiraish, N. Dontha, D. Lere and P. A. M. Farias, *J. Am. Chem. Soc.*, 1996, **118**, 7667.

Received in Cambridge, UK, 31st July 1997 (NCL Communication No. 6397); 7/05539K